eLIFE elifesciences.org

RESEARCH ARTICLE

Figures and figure supplements

ATRX promotes maintenance of herpes simplex virus heterochromatin during chromatin stress

Joseph M Cabral *et al*

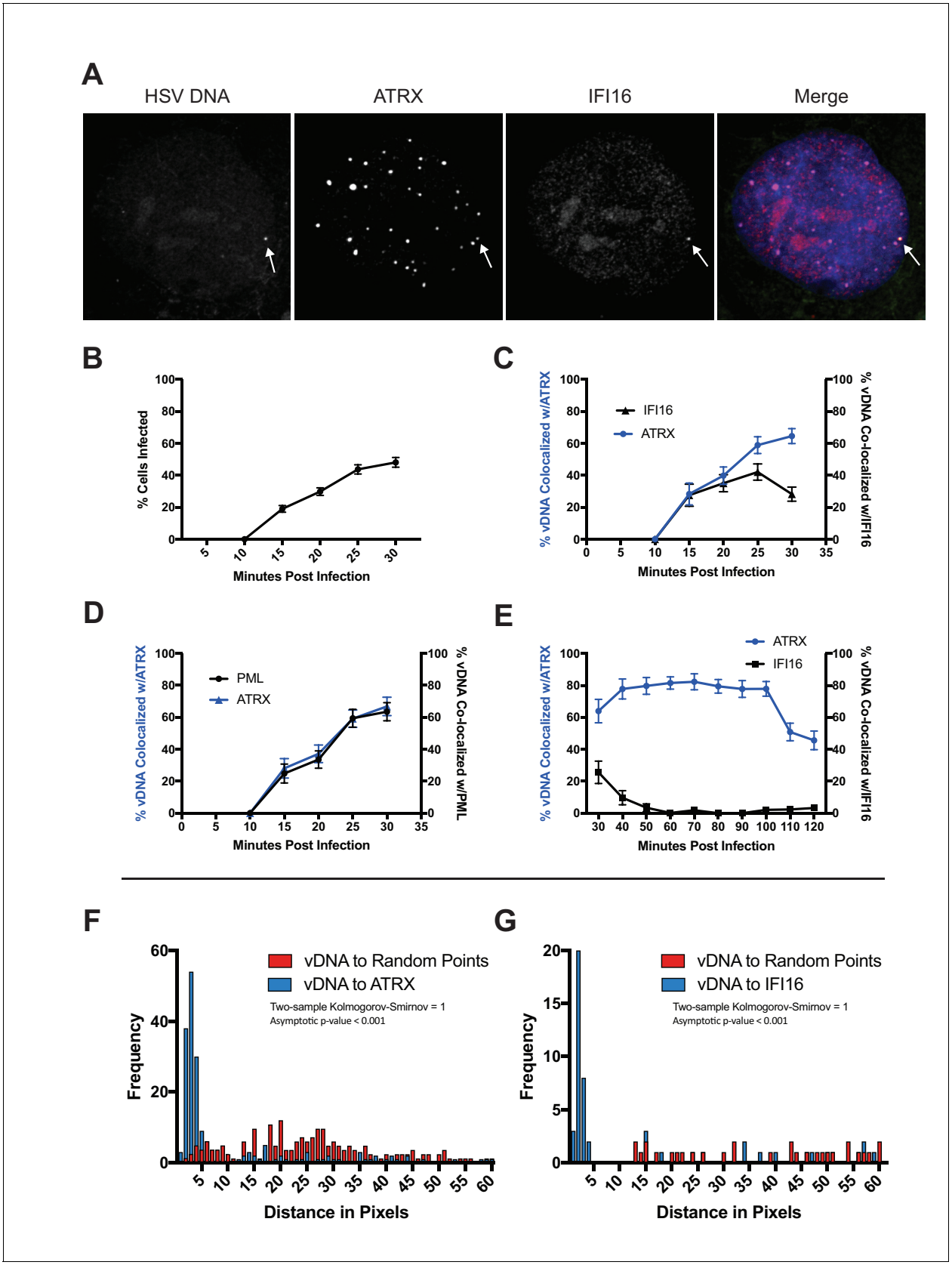

Figure 1. HSV genomes colocalize with host restriction factors upon nuclear entry. HFFs were infected with HSV-EdC at an MOI of 5 and fixed at times post infection as indicated. Host proteins were detected by immunocytochemistry, and HSV genomes were detected with click chemistry and a

Figure 1 continued on next page

Figure 1 continued

streptavidin-fluorophore probe. (**A**) Representative confocal image showing colocalization of ATRX and IFI16 with vDNA as indicated by the white arrows. (**B**) Percentage of cells with at least 1 HSV-EdC focus within the nucleus as determined by foci detection software. n ≥ 270 total cell population per time point from 15 to 30 mpi derived from 3 independent experiments. Percentage of vDNA foci colocalized with (**C**) ATRX (blue) or IFI16 (black) and (**D**) ATRX (blue) or PML (black) from 15 to 30 mpi in 5 min intervals as determined by foci detection and colocalization software (see Materials and methods). n ≥ 150 total cell population per time point from 15 to 30 mpi derived from 3 independent experiments. (**E**) Percentage of vDNA foci colocalized with ATRX (blue) or IFI16 (black) from 30 to 120 mpi in 10 min intervals as determined by foci detection and colocalization software. n ≥ 65 total cell population per time point from 30 to 120 mpi derived from 3 independent experiments. (**F**) Frequency distribution of distances from the center of a vDNA focus to the center of the nearest neighbor ATRX focus within a 60 pixel radius of the vDNA focus (blue) vs a distribution of distances from vDNA to randomly generated points within the nucleus equal to the number of ATRX foci (see ***Figure 1—figure supplement 1A***). Distance values were binned in increments of 1 pixel with the center of the first bin set to 0.5 pixels. Kolmogorov-Smirnov test was used to compare distributions and generate a p value. 0 = same underlying distribution, 1 = d distributions are significantly different (see Materials and methods). n = 183 vDNA foci. (**G**) Frequency distribution of distances (as in F) from the center of a vDNA focus to the center of an IFI16 focus vs vDNA to random points. n = 51 vDNA foci. All data are reported ± standard error of the mean.

DOI: https://doi.org/10.7554/eLife.40228.003

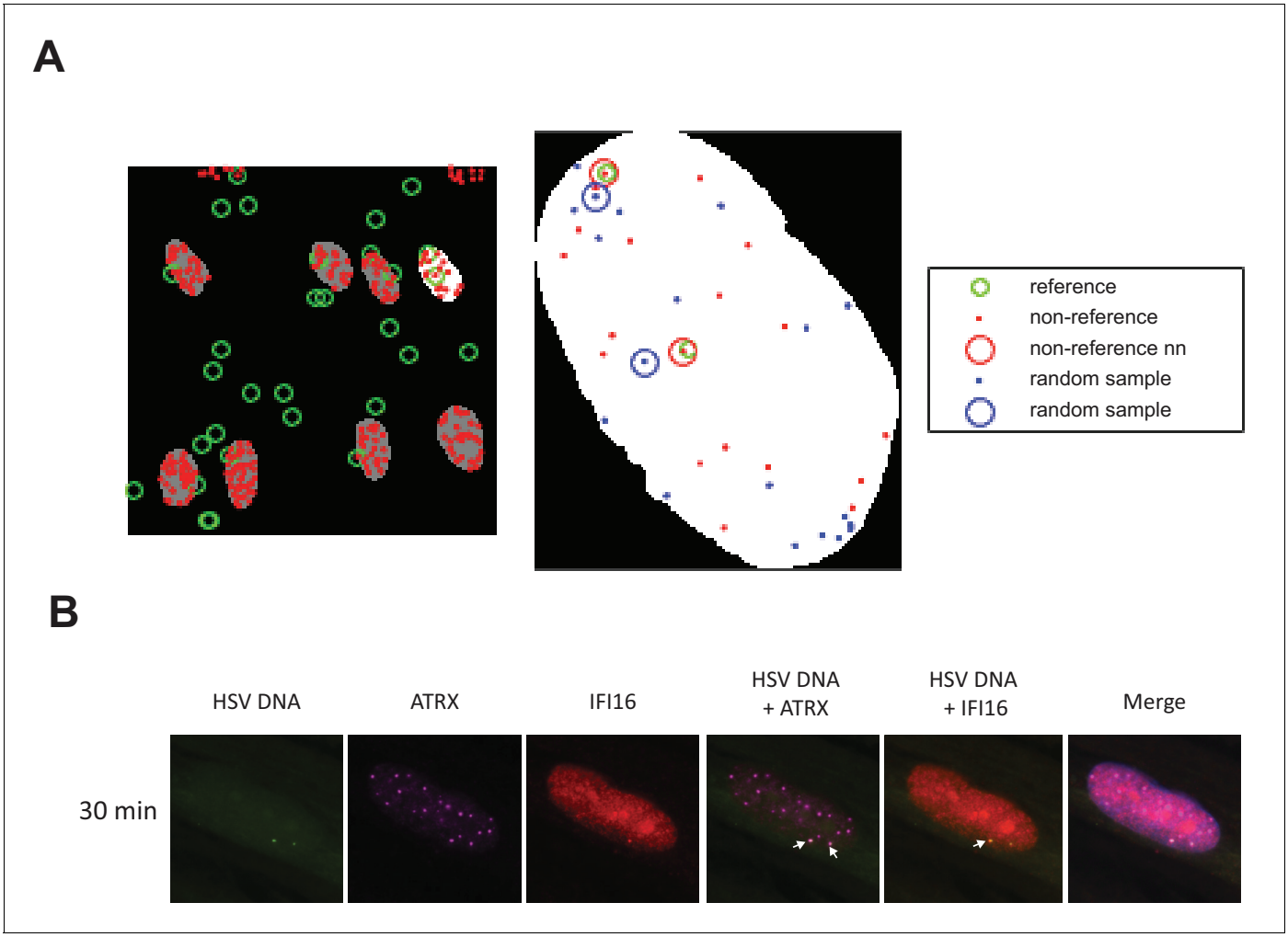

Figure 1—figure supplement 1. Foci and colocalization detection. (**A**) Screen shot from the frequency distribution script. For each reference channel focus (green) that is detected in a nuclear area (center), the script records the distance between the reference focus and its nearest neighbor (nn) non-reference focus (red). The script also generates random x,y positions within the nuclear mask to simulate the center of a random sample object (blue) and records the distance from the reference channel foci to random sample nn. The script generates a number of random sample points equal to the number of non-reference foci detected within that nuclear area. The script then generates a report of distances from each reference focus to its nearest neighbor in the non-random sample set and the random sample set within a defined radius from the reference focus. (**B**) Sample image showing ATRX (magenta) and IFI16 (red) colocalization with vDNA (green). White arrows indicate areas of colocalization.

DOI: https://doi.org/10.7554/eLife.40228.004

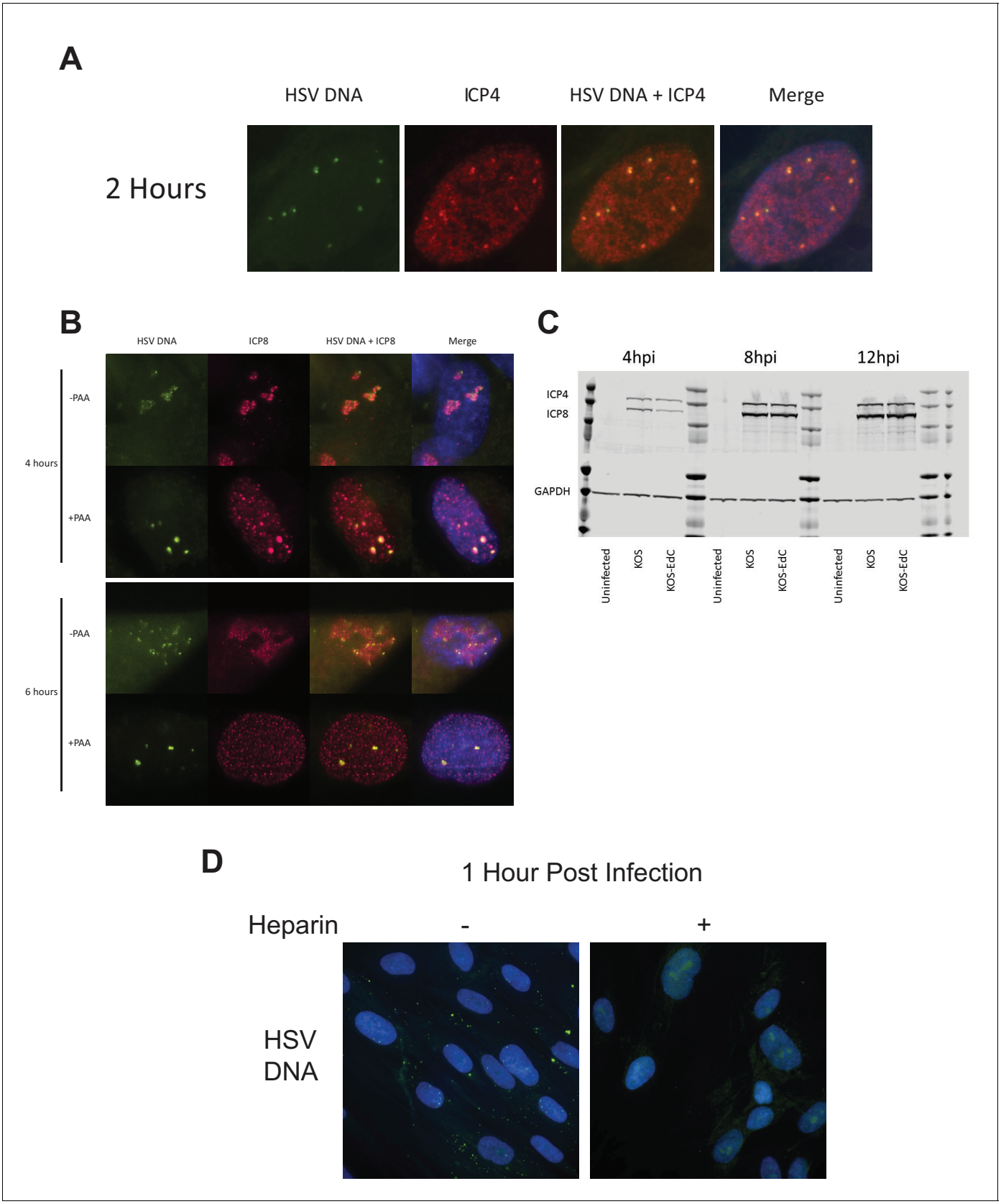

Figure 1—figure supplement 2. EdC labeling of KOS HSV. (**A**) HFF cells infected with HSV-EdC at an MOI of 5 and fixed at 2 hpi. vDNA is shown in green and viral protein ICP4 in red. (**B**) HFF cells infected with HSV-EdC at an MOI of 5 in the absence (-) or presence (+) of viral DNA synthesis inhibitor

Figure 1—figure supplement 2 continued on next page

Figure 1—figure supplement 2 continued

PAA and fixed at 4 and 6 hpi. vDNA is shown in green and viral protein ICP8 in red. (**C**) Immunoblot comparing ICP4 and ICP8 from HSV and HSV-EdC at 4, 8, and 12 hpi. (**D**) HFF cells infected with HSV-EdC at an MOI of 5 in the absence (-) or presence (+) heparin at 1 hpi. HSV-EdC genomes in green.
DOI: https://doi.org/10.7554/eLife.40228.005

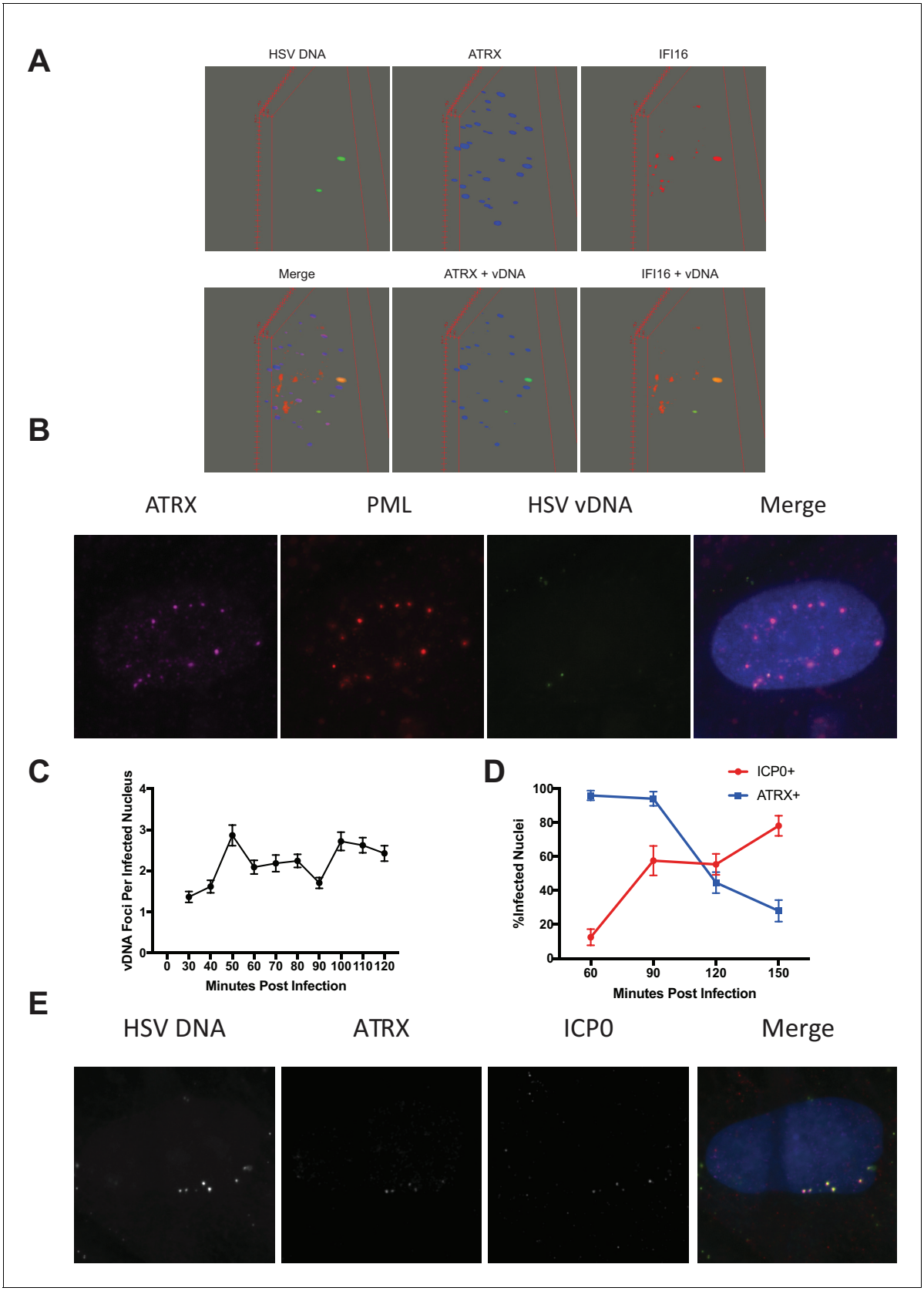

Figure 1—figure supplement 3. HSV DNA colocalization with ATRX, IFI16, and PML. (**A**) FIJI generated 3D volume projections of ATRX (blue) and IFI16 (red) colocalization with vDNA (green). Red lines define the bounding box of the X, Y, Z area being projected. (**B**) ATRX (magenta) and PML (red)

Figure 1—figure supplement 3 continued on next page

Figure 1—figure supplement 3 continued

colocalization with vDNA (green) at one hpi with HSV-EdC at an MOI of 5. (**C**) The number of viral DNA per infected nucleus from 30–120 mpi after infection with HSV-EdC at an MOI of 5. n ≥ 36 infected nuclei per time point. (**D**) Percentage of nuclei that are positive for HSV vDNA plus ATRX staining (ATRX+) or vDNA plus ICP0 staining (ICP0+) from 60–150 mpi. n ≥ 33 infected nuclei per time point. (**E**) HFFs infected with HSV-EdC at an MOI of 5. Cells were fixed and stained for HSV DNA, ATRX, and ICP0 at 90 mpi.

DOI: https://doi.org/10.7554/eLife.40228.006

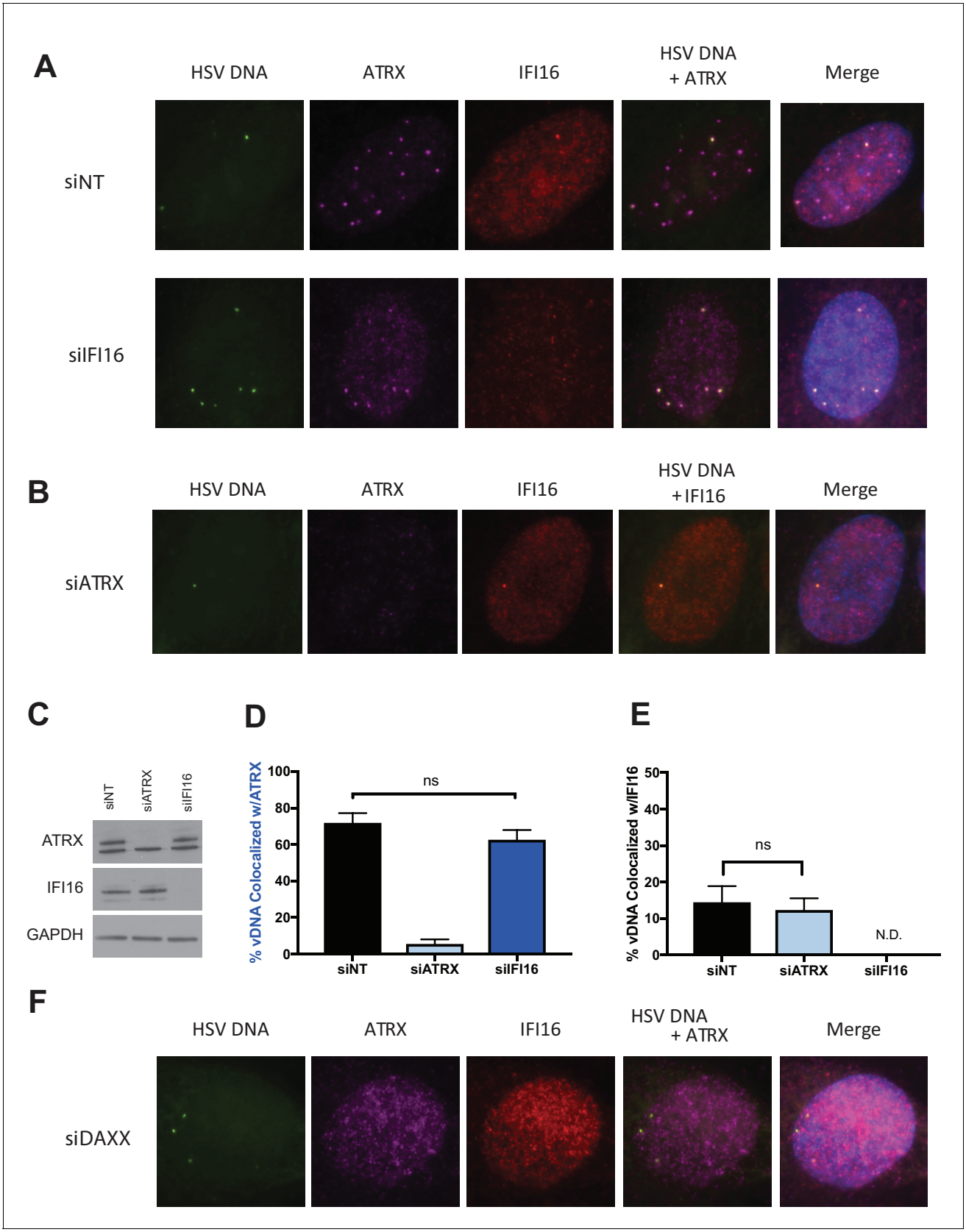

Figure 2. ATRX and IFI16 independently localize to viral DNA. HFFs were treated with siRNAs targeting ATRX (siATRX), IFI16 (siIFI16), DAXX (siDAXX), or non-targeting (siNT). 72 hr post siRNA treatment, cells were infected with HSV-EdC at an MOI of 5. (**A**) Colocalization of ATRX (magenta) and IFI16

Figure 2 continued on next page

Figure 2 continued

(red) with vDNA (green) in HSV-EdC infected HFFs treated with either siNT or siIFI16 at one hpi. (**B**) Colocalization of ATRX and IFI16 with vDNA in HSV-EdC infected HFFs treated with siATRX at 30 mpi. (**C**) Immunoblot detection of ATRX and IFI16 in lysates from HFFs treated with siRNA against either ATRX or IFI16 72 hr post treatment. GAPDH was used as a loading control. Percentage of vDNA that colocalizes with (**D**) ATRX or (**E**) IFI16 in cells treated with siNT, siATRX, or siIFI16 30 mpi as determined by foci detection and colocalization software. n $\geq$ 120 total cell population derived from two independent experiments, one-way ANOVA. All data are reported ± standard error of the mean. (**F**) Colocalization of ATRX and IFI16 with vDNA in HSV-EdC infected HFFs treated with siDAXX at 30 mpi.

DOI: https://doi.org/10.7554/eLife.40228.008

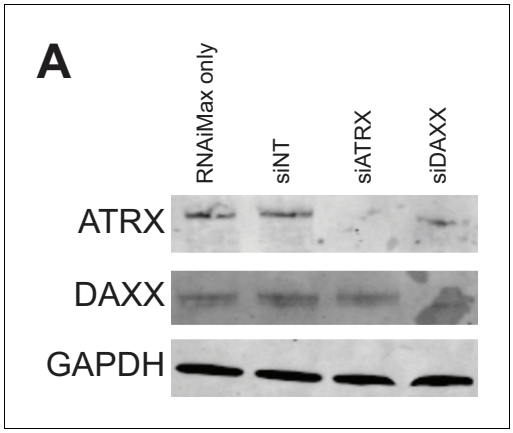

Figure 2—figure supplement 1. siRNA depletion of ATRX and DAXX in HFF cells. (**A**) Immunoblot detection of ATRX and DAXX from HFF whole cell lysates 72 h after treatment with transfection reagent only (RNAiMax only), siNT, siATRX, siDAXX, or siATRX + siDAXX (siA+D).

DOI: https://doi.org/10.7554/eLife.40228.009

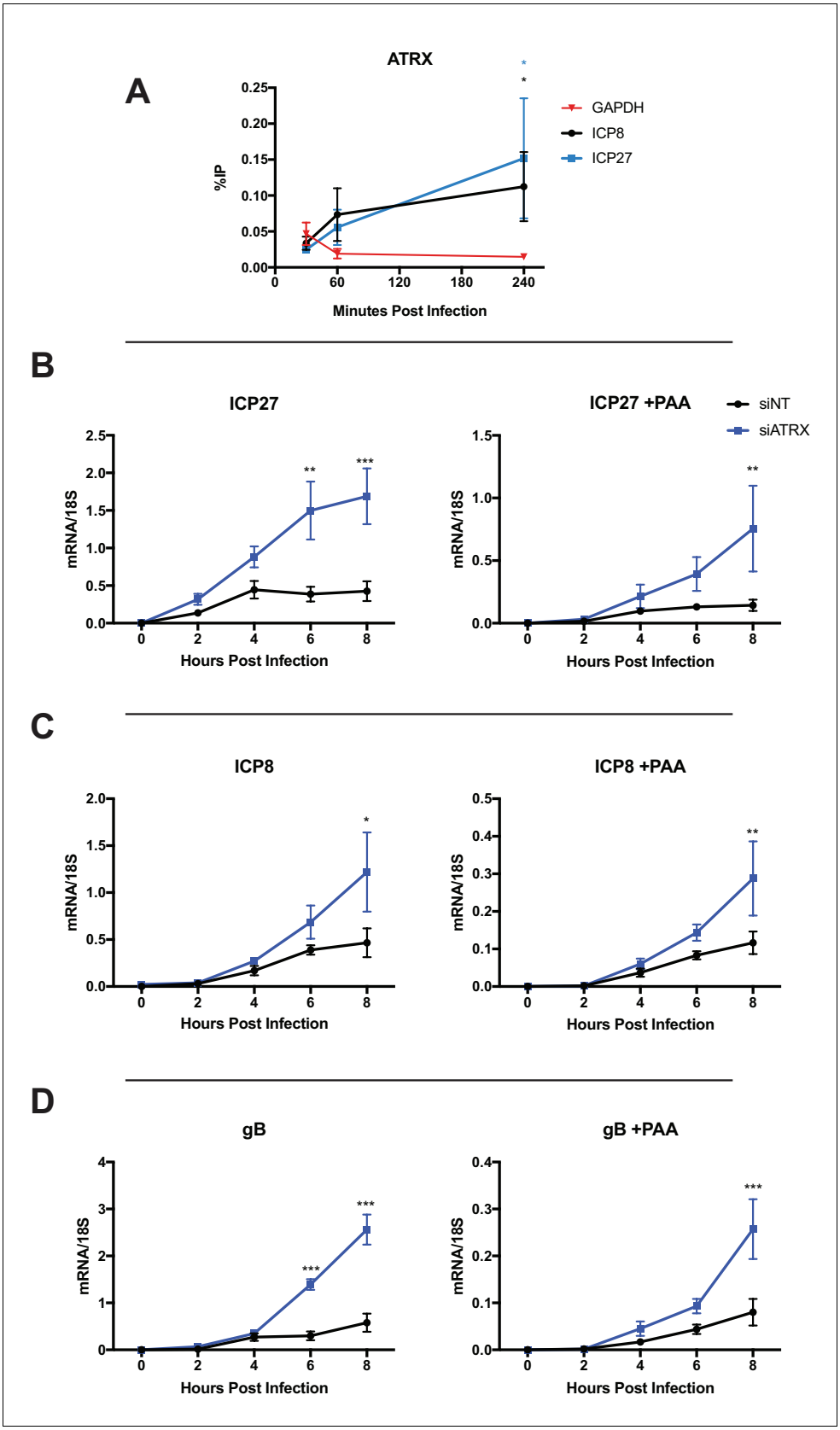

Figure 3. ATRX restricts HSV gene expression from input and progeny viral DNA. (**A**) HFFs were infected with HSV 7134 at an MOI of 3, and infected cells were fixed and harvested 30, 60, and 240 min post infection. ChIP-qCPR and HSV specific primers were used to detect chromatin enrichment of

Figure 3 continued on next page

Figure 3 continued

ATRX at ICP27 (blue) and ICP8 (black) gene promoters. Two-tailed t-tests were used to compare ATRX enrichment at viral gene promoters compared to GAPDH. (**B**) HFFs were treated with siNT or siATRX and infected with HSV 7134 at an MOI of 5 in the absence (left panels) or presence (right panels) of PAA. Relative viral transcripts for (**B**) *ICP27*, (**C**) *ICP8*, or (**D**) *gB* were quantified by qPCR at 0, 2, 4, 6, and 8 hpi. Viral mRNA levels were normalized to cellular 18S transcripts. Results were analyzed by two-way ANOVA. All data for ***Figure 3*** are reported as the average of 3 independent experiments ± standard error of the mean; $p < 0.05$ (*), $p < 0.01$ (**), $p < 0.001$ (***).

DOI: https://doi.org/10.7554/eLife.40228.010

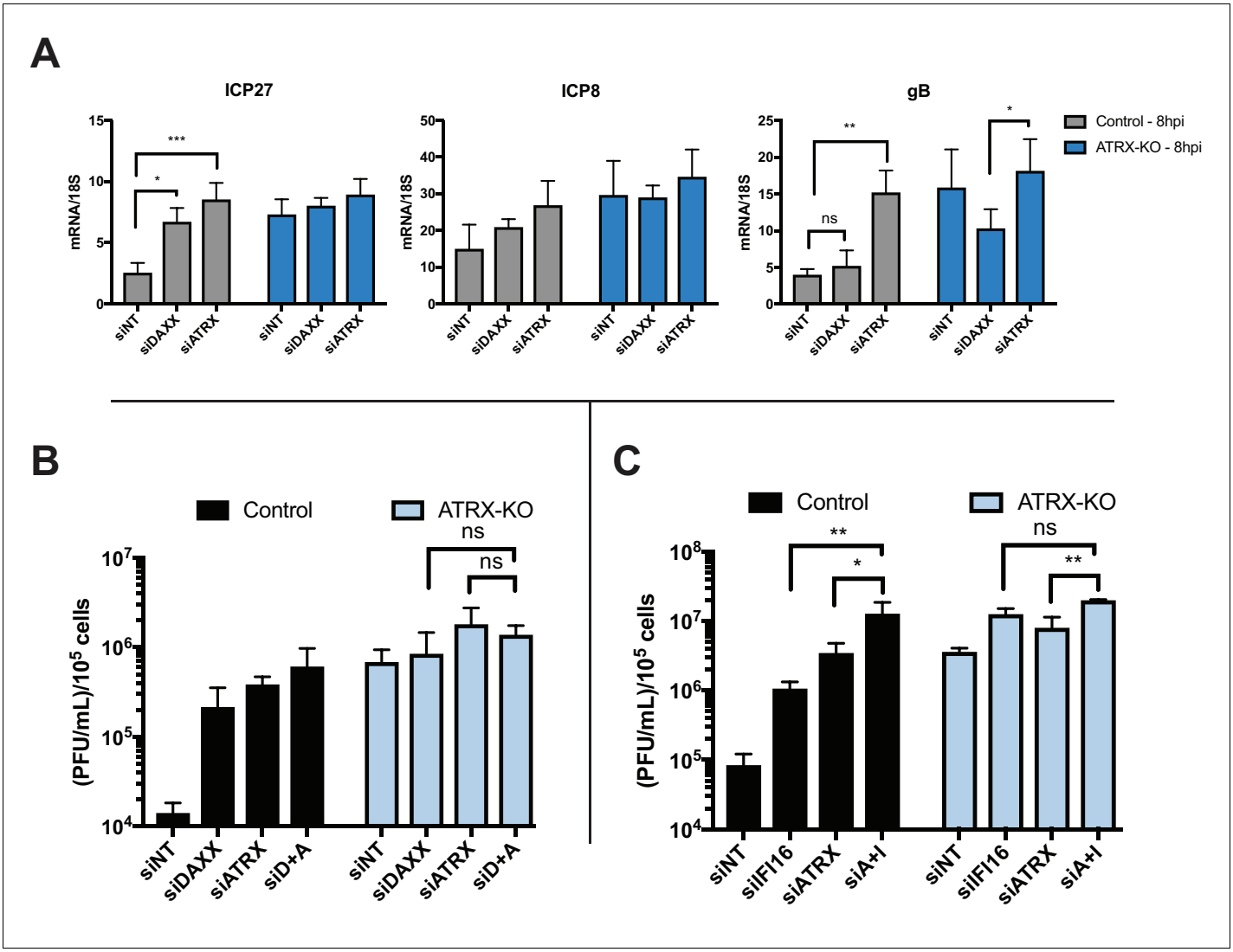

Figure 4. ATRX and DAXX cooperatively restrict HSV gene expression via an IFI16-independent pathway. (**A**) Relative viral transcripts for *ICP27*, *ICP8*, and *gB* detected by qPCR in whole cell lysates collected from ATRX-KO or Control cells treated with siNT, siDAXX, or siATRX for 72 hr then infected with HSV 7134 at an MOI of 5. Lysates were collected at 4 and 8 hpi. Results were analyzed by two-way ANOVA. (**B**) Viral yields from ATRX-KO and Control cells treated with siRNAs against non-targeting, ATRX, DAXX, or ATRX +DAXX (siD +A) and infected with HSV 7134 at an MOI of 0.1. Viral lysates were collected at 24 hpi and titrated on U2OS cells. Yields were normalized to (PFU/mL)/1 $\times$ 10^5 cells. Results were analyzed by two-way ANOVA. (**C**) Viral yields from ATRX-KO and Control cells treated with siRNAs against non-targeting, ATRX, IFI16, or ATRX + IFI16 (siA + I) and infected with HSV 7134 at an MOI of 0.1. Viral lysates were collected at 48 hpi and titrated on U2OS cells. Yields were normalized to (PFU/mL)/1 $\times$ 10^5 cells. Results were analyzed by two-way ANOVA. All data for ***Figure 4*** are reported as the average of 3 independent experiments ± standard error of the mean; $p < 0.05$ (*), $p < 0.01$ (**), $p < 0.001$ (***).

DOI: https://doi.org/10.7554/eLife.40228.011

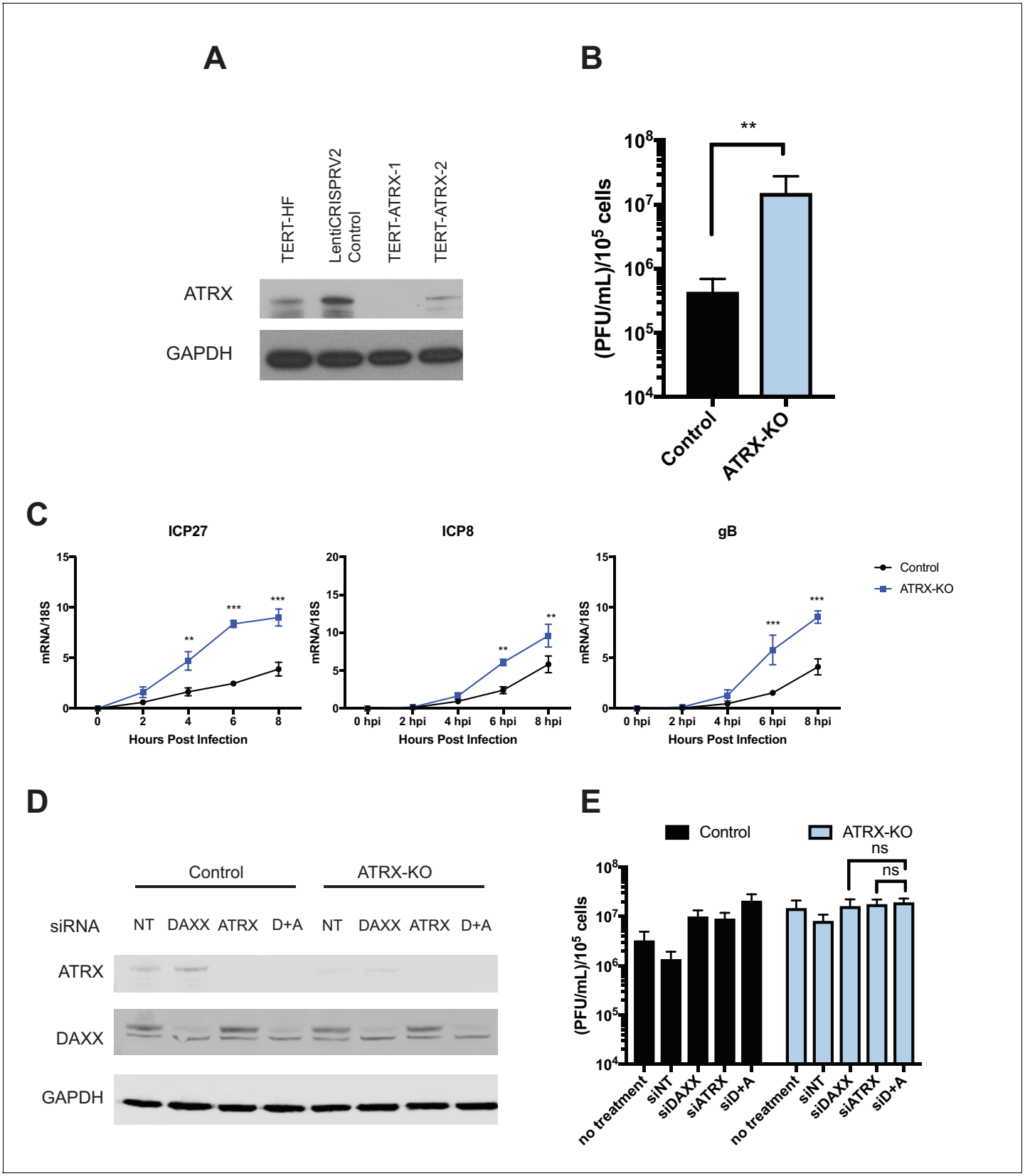

Figure 4—figure supplement 1. CRISPR-mediated knockout of ATRX alleviates viral restriction. (**A**) Immunoblot of immortalized fibroblasts (TERT-HF) transduced with lentivirus expressing Cas9 alone (LenitCRISPR V2 control), or Cas9 and co-expressing sgRNA against ATRX (TERT-ATRX-1 and TERT-

Figure 4—figure supplement 1 continued on next page

Figure 4—figure supplement 1 continued

ATRX-2). LenitCRISPR V2 control was used as the Control cell line in this study. TERT-ATRX-1 was used as the ATRX-KO cell line in this study. (**B**) Viral yields from Control and ATRX-KO cells infected with HSV 7134 at an MOI of 0.1 for 48 hr. Viral lysates were collected and titrated on U2OS cells. Yields were normalized to (PFU/mL)/1 × 105 cells. Results analyzed by two-tailed t-test. (**C**) Relative viral transcripts for *ICP27*, *ICP8*, and *gB* detected by qPCR in whole cell lysates collected from ATRX-KO or Control cells treated with siNT, siDAXX, or siATRX for 72 hr then infected with HSV 7134 at an MOI of 5. Lysates were collected at 4 and 8 hpi. Results were analyzed by two-way ANOVA. (**D**) Control and ATRX-KO cells treated with siNT, siDAXX, siATRX, or siATRX + siDAXX (siA + D). (**E**) Viral yields from ATRX-KO and Control cells treated with siRNAs against non-targeting, ATRX, DAXX, or ATRX + DAXX (siD + A) and infected with HSV 7134 at an MOI of 3. Results were analyzed by two-way ANOVA. Panels B, C, and E are reported as the average of 3 independent experiments ± standard error of the mean; $p < 0.05$ (*), $p < 0.01$ (**), $p < 0.001$ (***).

DOI: https://doi.org/10.7554/eLife.40228.012

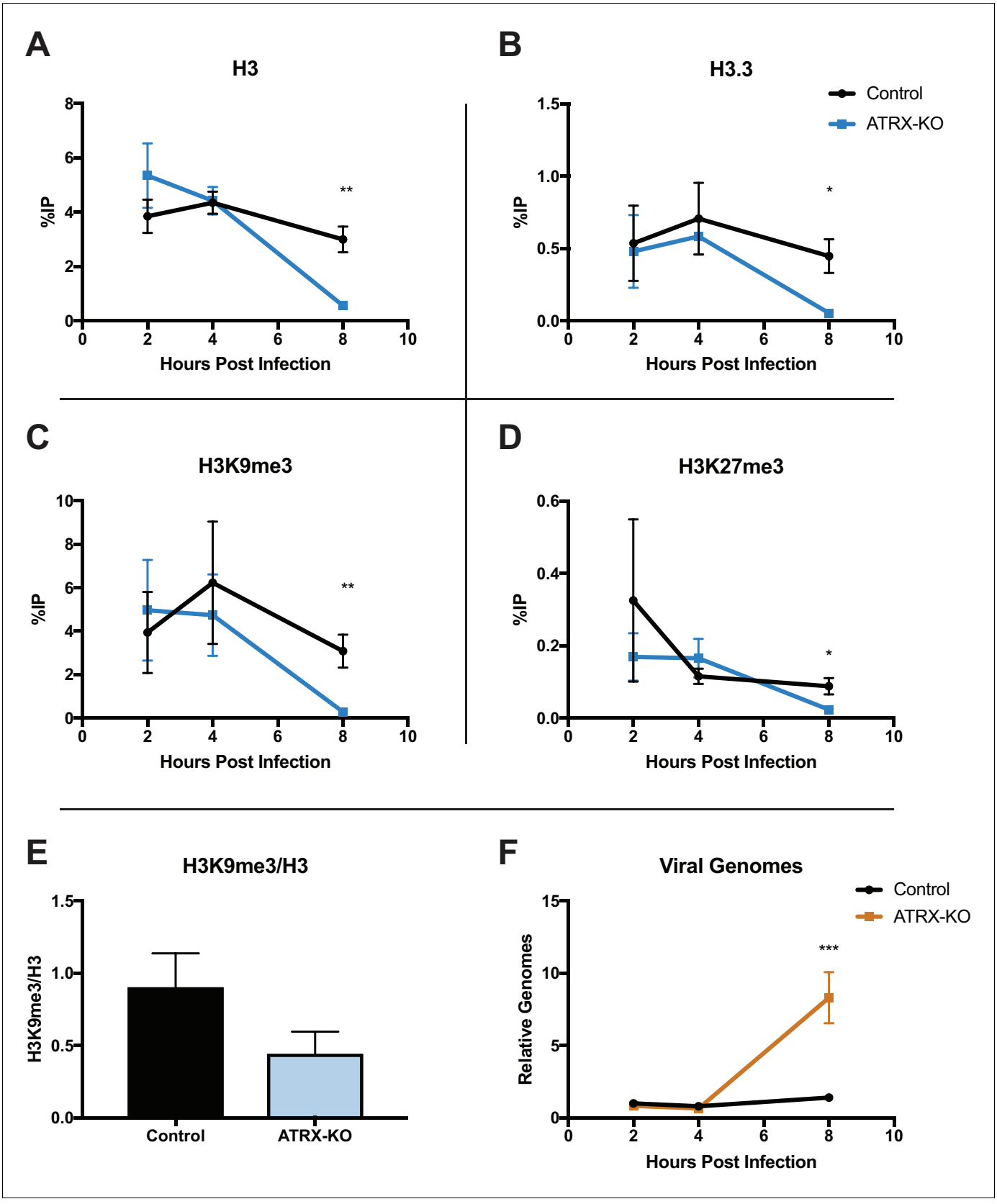

Figure 5. ATRX depletion enhances ICP0-null HSV DNA Replication and removal of heterochromatin. ATRX-KO or Control cells were infected with HSV 7134 at an MOI of 3. Infected cells were fixed and harvested 2, 4, and 8 hpi. ChIP-qCPR and HSV specific primers were used to detect chromatin

Figure 5 continued on next page

Figure 5 continued

enrichment of (**A**) H3, (**B**) H3.3, (**C**) H3K9me3, and (**D**) H3K27me3 at the viral gene promoter for *ICP27*. Results are reported as the percent of input immunoprecipitated by each antibody. Two-tailed t-tests were used to compare results from ATRX-KO versus Control cells for each antibody and each time point. (**E**) H3K9me3 enrichment per H3 for the *ICP27* promoter. (**F**) Chromatin input for *ICP8* relative to input *GAPDH* to determine relative viral genome copy numbers. All data for ***Figure 5*** are reported as the average of 4 independent experiments ± standard error of the mean; $p < 0.05$ (*), $p < 0.01$ (**).

DOI: https://doi.org/10.7554/eLife.40228.013

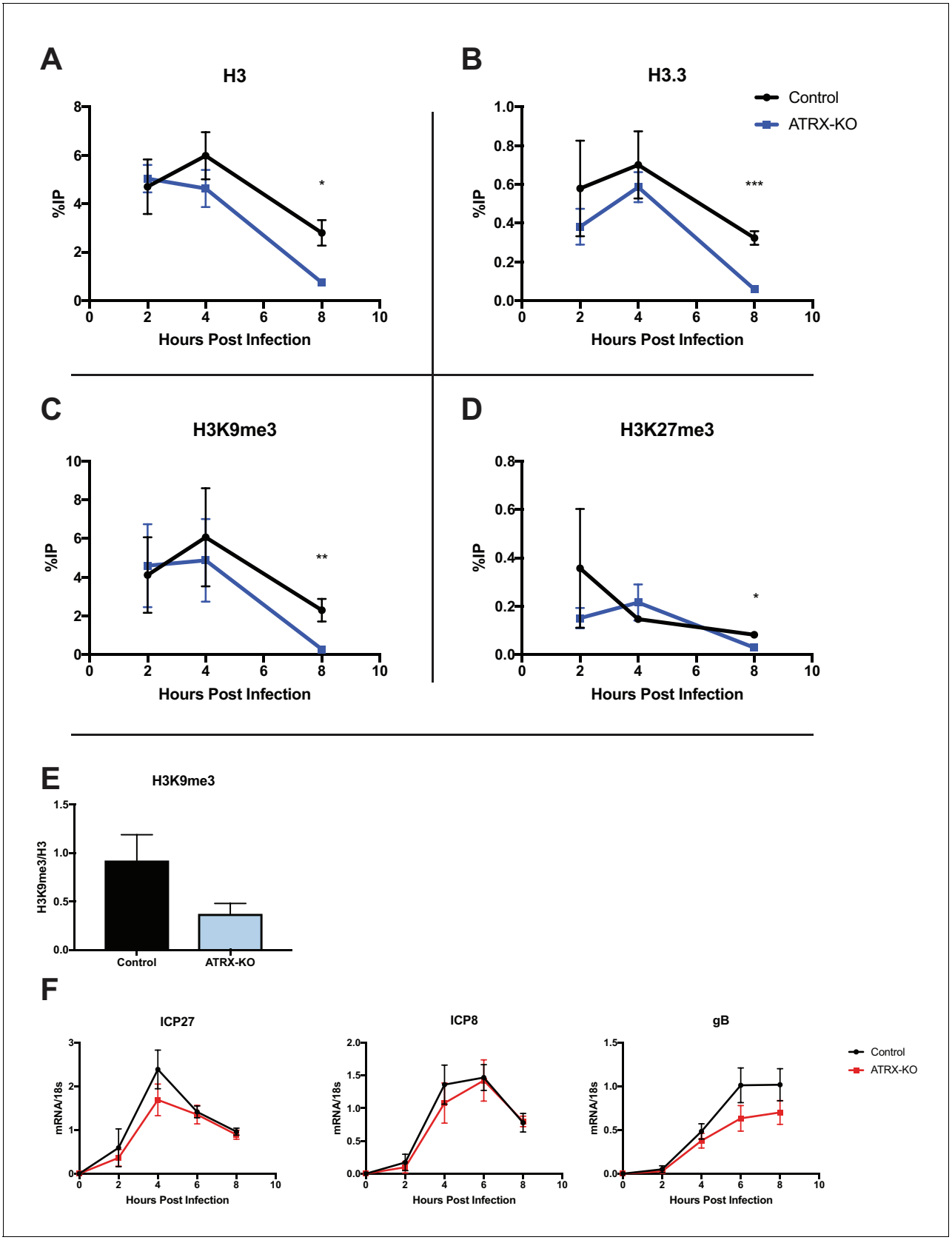

Figure 5—figure supplement 1. ATRX depletion enhances removal of heterochromatin from the ICP8 promoter. ATRX-KO or Control cells were infected with HSV 7134 at an MOI of 3. Infected cells were fixed and harvested 2, 4, and 8 hpi. ChIP-qCPR and HSV specific primers were used to

Figure 5—figure supplement 1 continued on next page

Figure 5—figure supplement 1 continued

detect chromatin enrichment of (**A**) H3, (**B**) H3.3, (**C**) H3K9me3, and (**D**) H3K27me3 at the viral gene promoter for *ICP8*. Results are reported as the percent of input immunoprecipitated by each antibody. Two-tailed t-tests were used to compare results from ATRX-KO versus Control cells for each antibody and each time point. (**E**) H3K9me3 enrichment per H3 for the *ICP8* promoter. ChIP-PCR experiments in ***Figure 5—figure supplement 1*** are reported as the average of 4 independent experiments ± standard error of the mean; $p < 0.05$ (*), $p < 0.01$ (**). (**F**) Relative viral transcripts for *ICP27*, *ICP8*, and *gB* detected by qPCR in whole cell lysates collected from ATRX-KO or Control cells that were infected with HSV 7134R at an MOI of 5. Lysates were collected at 0, 2, 4, 6, and 8 hpi. Viral mRNA was normalized to cellular 18S transcripts.

DOI: https://doi.org/10.7554/eLife.40228.014

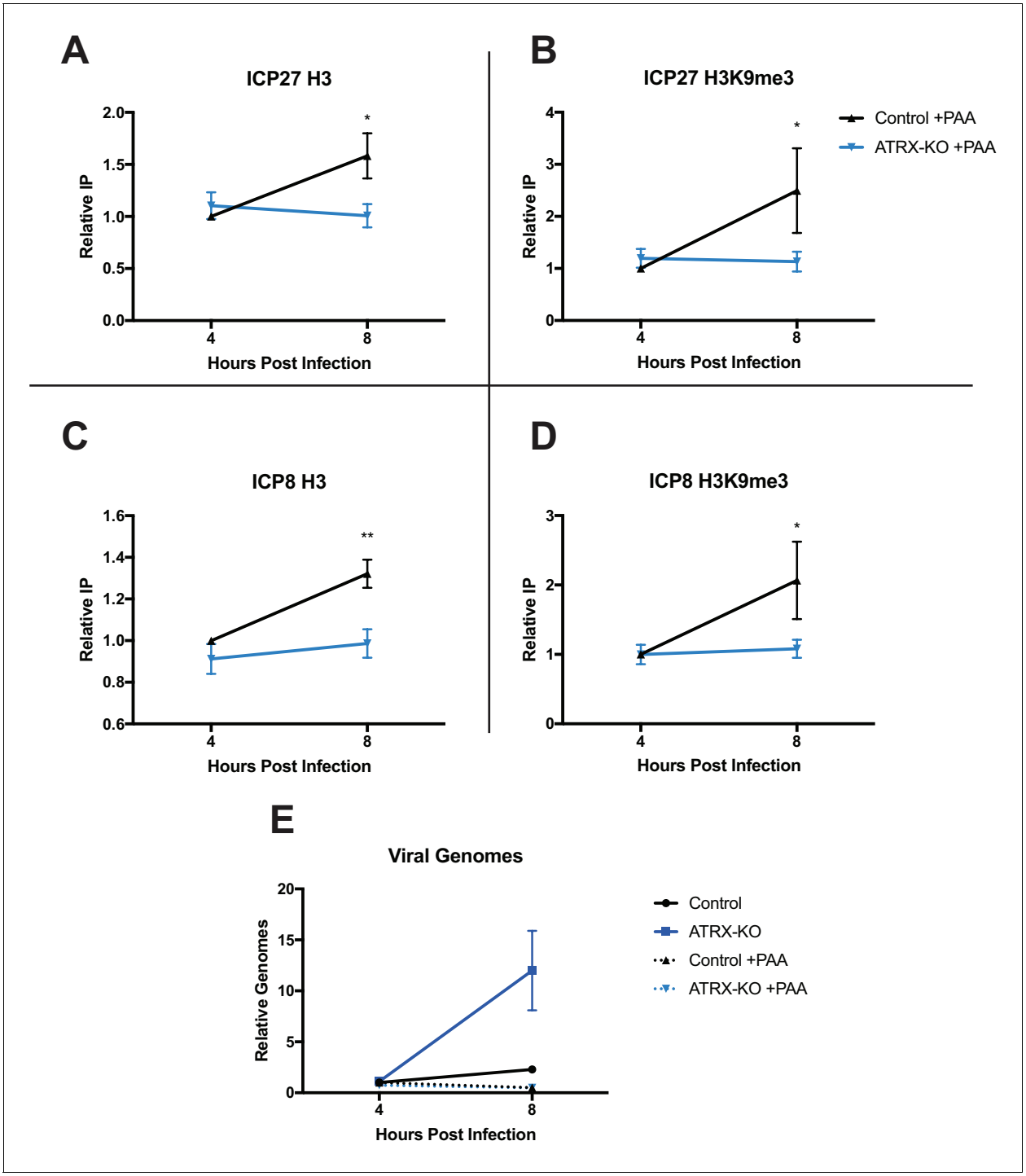

Figure 6. ATRX promotes maintenance of heterochromatin on input viral genomes. ATRX-KO or Control cells were infected with HSV 7134 at an MOI of 3. Infected cells were fixed and harvested 8 hpi. ChIP-qCPR and HSV specific primers were used to detect chromatin enrichment of at the viral gene promoters in the absence (***Figure 6—figure supplement 1A–D***) or presence of PAA. Enrichment of (**A**) H3 and (**B**) H3K9me3 at the *ICP27* gene promoter. Enrichment of (**C**) H3 and (**D**) H3K9me3 at the *ICP8* gene promoter. Results reported as Relative IP (the percent of input immunoprecipitated by each antibody normalized to the 4 hr control sample - set to 1.0 for each replicate). (**E**) Chromatin input for *ICP8* relative to input *GAPDH* to determine relative viral genome copy numbers in the absence or presence of PAA. All data for ***Figure 6*** are reported as the average of 4 independent experiments ± standard error of the mean; two-tailed t-test, $p < 0.05$ (*), $p < 0.01$ (**).

DOI: https://doi.org/10.7554/eLife.40228.015

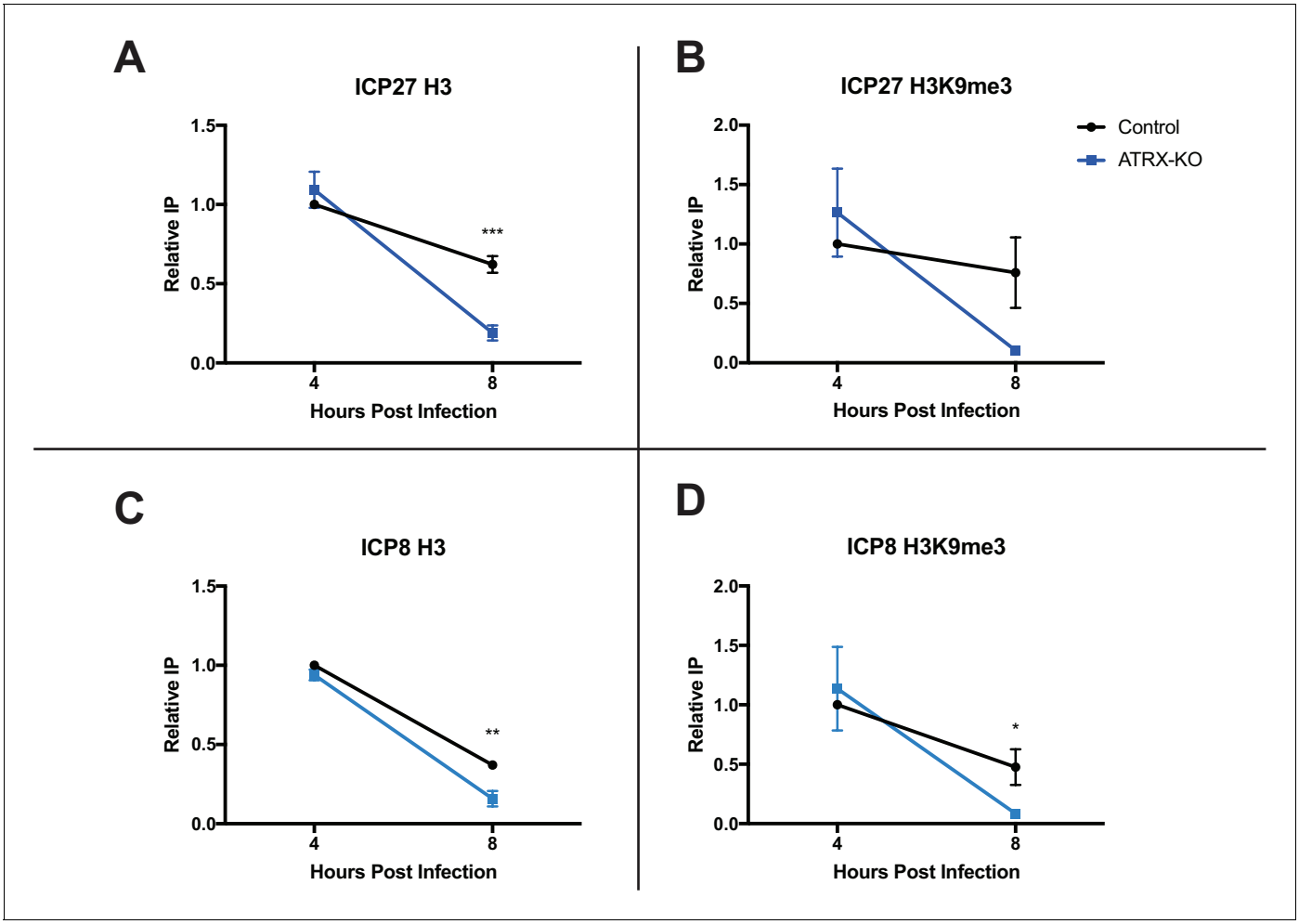

Figure 6—figure supplement 1. Untreated controls for ChIP. ATRX-KO or Control cells were infected with HSV 7134 at an MOI of 3. Infected cells were fixed and harvested 8 hpi. ChIP-qCPR and HSV specific primers were used to detect chromatin enrichment of at the viral gene promoters in the absence (this figure) or presence of PAA (***Figure 6***). Enrichment of (**A**) H3 and (**B**) H3K9me3 at the *ICP27* gene promoter. Enrichment of (**C**) H3 and (**D**) H3K9me3 at the *ICP8* gene promoter. Results are reported as 'Relative IP' (the percent of input immunoprecipitated by each antibody normalized to the 4 hr control sample set to 1.0 for each replicate). All data for ***Figure 6*** are reported as the average of 4 independent experiments ± standard error of the mean; two-tailed t-test, $p < 0.05$ (*), $p < 0.01$ (**), $p < 0.001$ (***).

DOI: https://doi.org/10.7554/eLife.40228.016

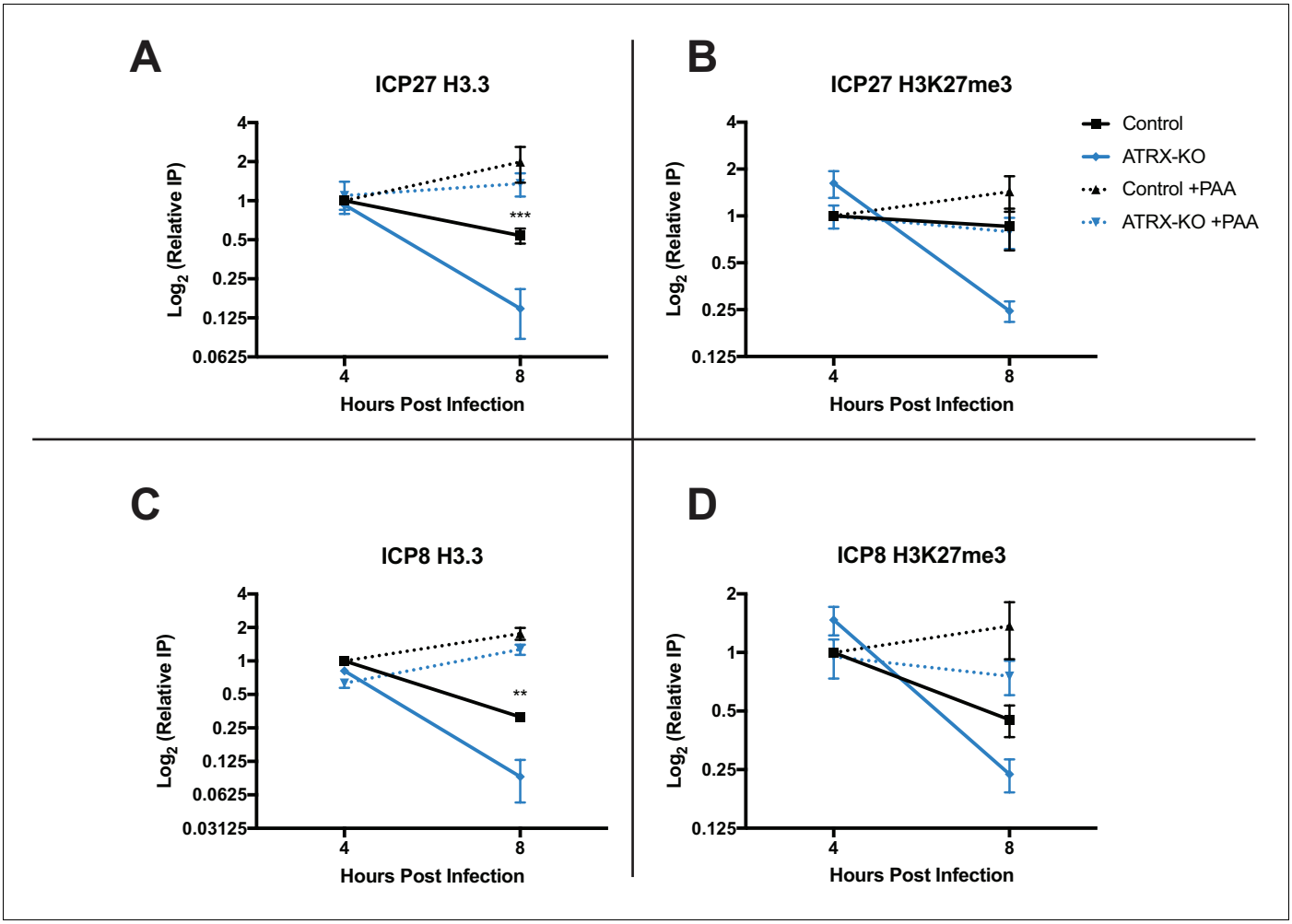

Figure 6—figure supplement 2. ATRX promotes maintenance of H3K27me3 and H3.3 on input viral genomes. ATRX-KO or Control cells were infected with HSV 7134 at an MOI of 3. Infected cells were fixed and harvested 8 hpi. ChIP-qCPR and HSV specific primers were used to detect chromatin enrichment of at the viral gene promoters in the absence (solid lines) or presence (dotted lines) of PAA. Enrichment of (**A**) H3.3 and (**B**) H3K27me3 at the *ICP27* gene promoter. Enrichment of (**C**) H3.3 and (**D**) H3K27me3 at the *ICP8* gene promoter. Results are reported as 'Relative IP' (the percent of input immunoprecipitated by each antibody normalized to the 4 hr control sample set to 1.0 for each replicate). All data for ***Figure 6*** are reported as the average of 4 independent experiments ± standard error of the mean; two-tailed t-test, $p < 0.05$ (*), $p < 0.01$ (**), $p < 0.001$ (***).

DOI: https://doi.org/10.7554/eLife.40228.017

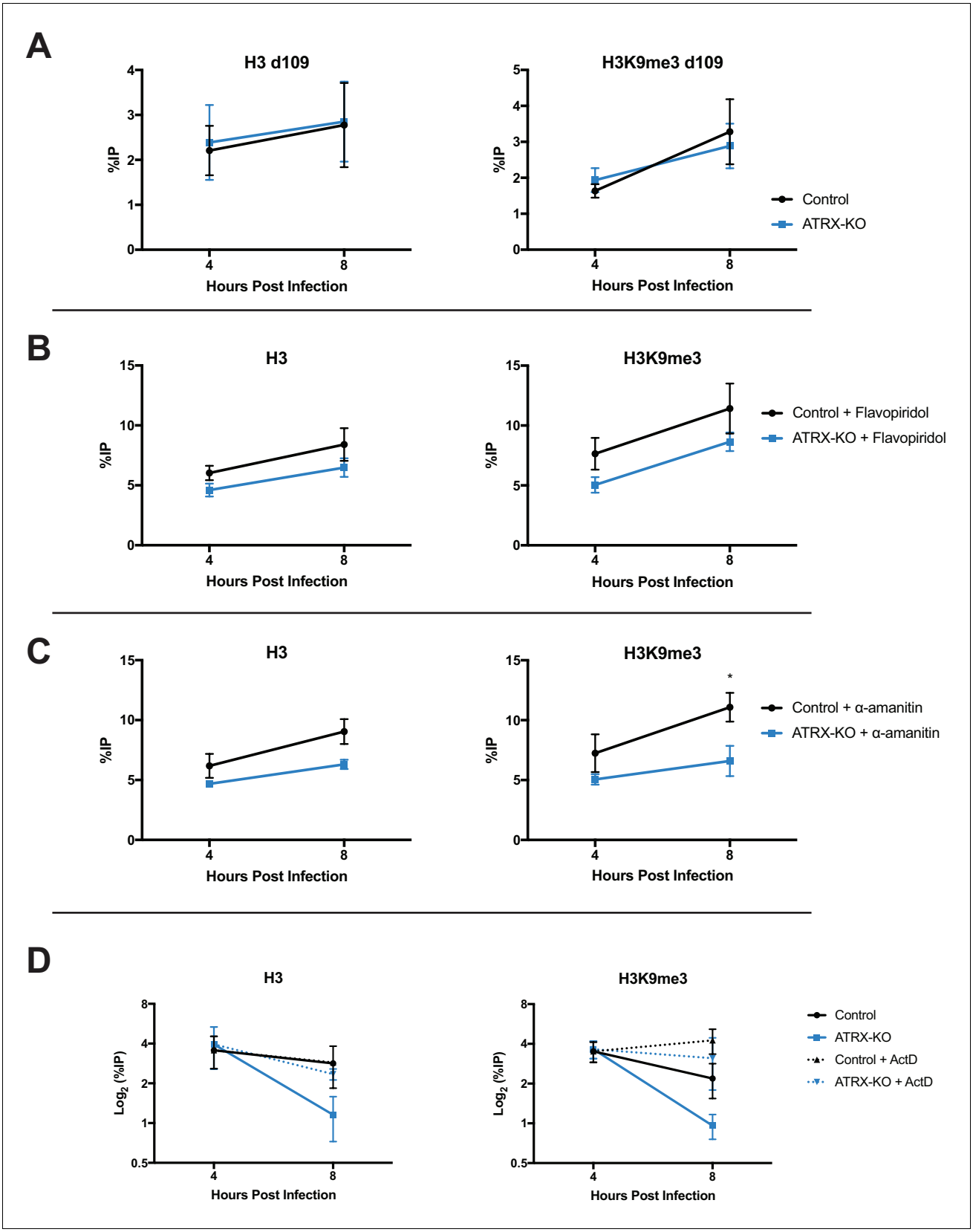

Figure 7. ATRX promotes heterochromatin maintenance during challenges to chromatin stability. (**A**) ATRX-KO and Control cells were infected with HSV *d*109 at an MOI of 3 and fixed and harvested at 4 and 8 hpi. ChIP-qPCR was used to detect H3 and H3K9me3 enrichment at the *ICP8* promoter. (**B**)

Figure 7 continued on next page

Figure 7 continued

ATRX-KO and Control cells were treated with flavopiridol (flavopiridol; 1 μM) from 1 hr prior to infection until time of harvest. Treated and untreated (***Figure 7—figure supplement 1A–B***) cells were infected with HSV 7134 at MOI three and fixed at 4 and 8 hpi. ChIP-qPCR was used to detect H3 and H3K9me3 enrichment at the *ICP8* promoter. (**C**) ATRX-KO and Control cells were treated with α-amanitin (2 μg/mL) from 16 hr prior to infection until time of harvest. Treated and untreated (***Figure 7—figure supplement 1C–D***) cells were infected with HSV 7134 at MOI three and fixed at 4 and 8 hpi. ChIP-qPCR was used to detect H3 and H3K9me3 enrichment at the *ICP8* promoter. (**D**) ATRX-KO and Control cells were infected with HSV 7134 at a MOI of 3 and treated with ActD (5 μg/mL) at 4 hpi. Samples were fixed and collected a 4 and 8 hpi. Chromatin enrichment is reported as percent input immunoprecipitated by antibodies specific for H3 and H3K9me3 as detected by qPCR using specific primers for the promoter of *ICP8*. All data for ***Figure 7*** are reported as the percent of input immunoprecipitated by each antibody and are the average of 3 independent experiments ± standard error of the mean; two-tailed t-test, $p < 0.05$ (*).

DOI: https://doi.org/10.7554/eLife.40228.018

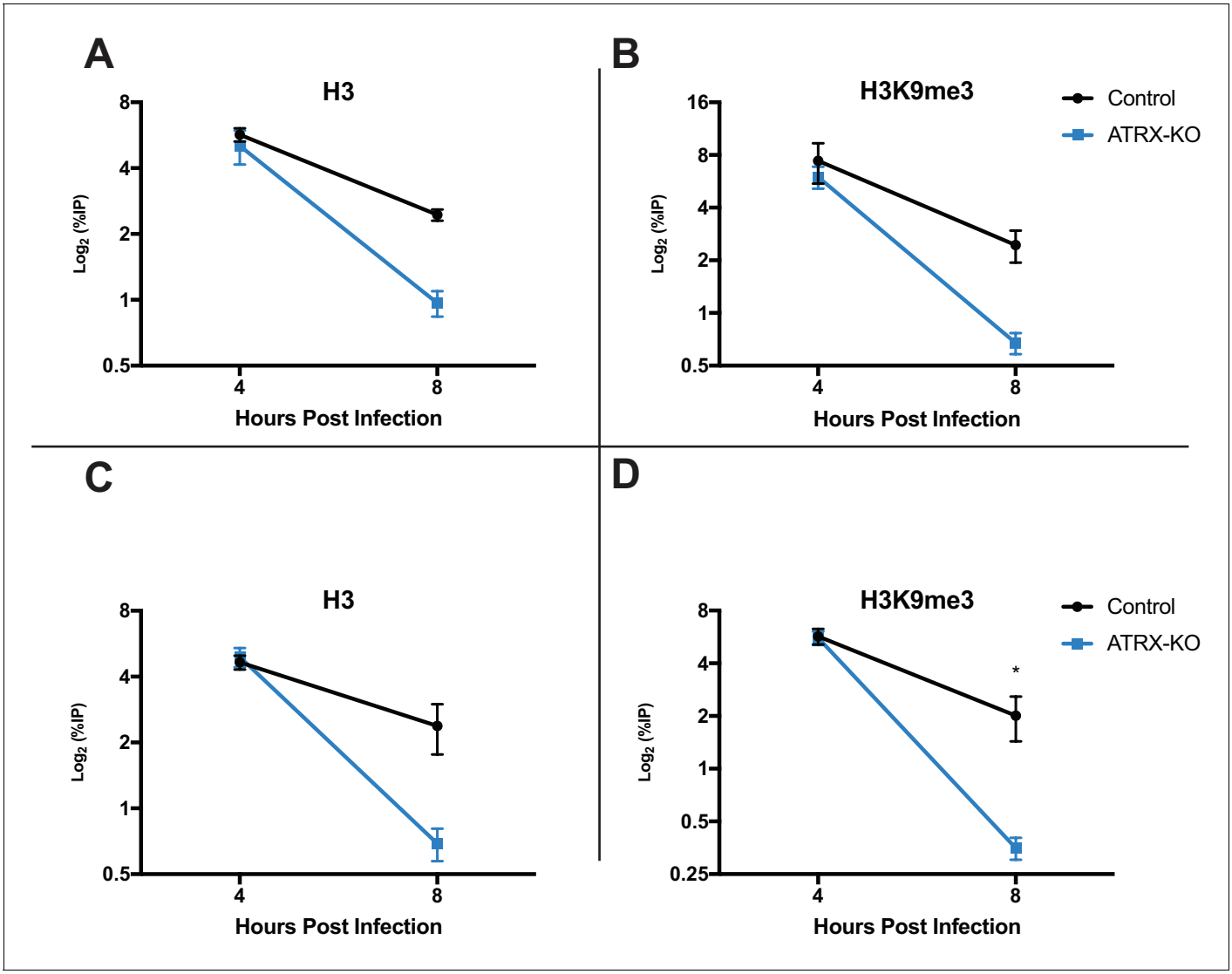

Figure 7—figure supplement 1. Untreated controls for flavopiridol and α-amanitin ChIPs. ATRX-KO and Control cells, not treated with flavopiridol, were infected with HSV 7134 at MOI three and fixed at 4 and 8 hpi as controls for ***Figure 7B***. ChIP-qPCR was used to detect (**A**) H3 and (**B**) H3K9me3 enrichment at the *ICP8* promoter. ATRX-KO and Control cells, not treated with α-amanitin, were infected with HSV 7134 at MOI three and fixed at 4 and 8 hpi as controls for ***Figure 7C***. ChIP-qPCR was used to detect (**C**) H3 and (**D**) H3K9me3 enrichment at the *ICP8* promoter. All data for ***Figure 7*** are reported as the percent of input immunoprecipitated by each antibody and are the average of 3 independent experiments ± standard error of the mean; two-tailed t-test, $p < 0.05$ (*).

DOI: https://doi.org/10.7554/eLife.40228.019

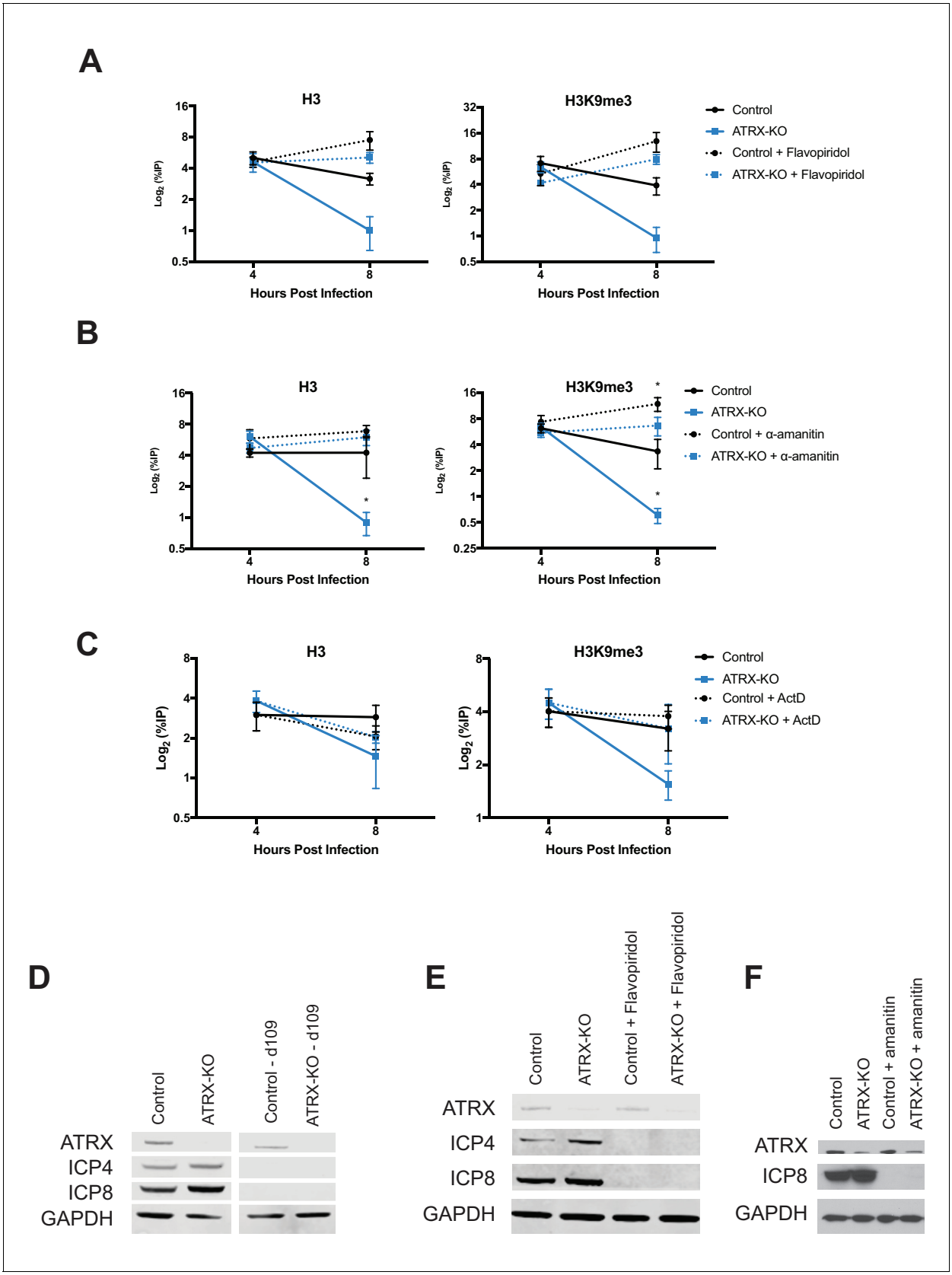

Figure 7—figure supplement 2. ATRX promotes heterochromatin maintenance at the ICP27 promoter during chromatin stress. (**A**) ATRX-KO and Control cells were treated with flavopiridol (flavopiridol; 1 μM) from 1 hr prior to infection until time of harvest. Treated cells were infected with HSV

Figure 7—figure supplement 2 continued on next page

Figure 7—figure supplement 2 continued

7134 at MOI three and fixed at 4 and 8 hpi. ChIP-qPCR was used to detect H3 and H3K9me3 enrichment at the *ICP27* promoter. (**B**) ATRX-KO and Control cells were treated with α-amanitin (2 μg/mL) from 16 hr prior to infection until time of harvest. Treated cells were infected with HSV 7134 at MOI three and fixed at 4 and 8 hpi. ChIP-qPCR was used to detect H3 and H3K9me3 enrichment at the *ICP27* promoter. (**C**) ATRX-KO and Control cells were infected with HSV 7134 at an MOI of 3 and treated with ActD (5 μg/mL) at 4 hpi. Samples were fixed and collected a 4 and 8 hpi. Chromatin enrichment is reported as percent input immunoprecipitated by antibodies specific for H3 and H3K9me3 as detected by qPCR using specific primers for the promoter of *ICP27*. (**D**) Immunoblot showing inhibition of ICP8 production in Control and ATRX-KO cells infected with HSV *d*109. (**E**) Immunoblot showing inhibition of ICP8 production in Control and ATRX-KO cells when treated with flavopiridol. (**F**) Immunoblot showing inhibition of ICP8 production in Control and ATRX-KO cells when treated with α-amanitin. All data for ***Figure 7*** are reported as the percent of input immunoprecipitated by each antibody and are the average of 3 independent experiments ± standard error of the mean; two-tailed t-test, $p < 0.05$ (*).
DOI: https://doi.org/10.7554/eLife.40228.020

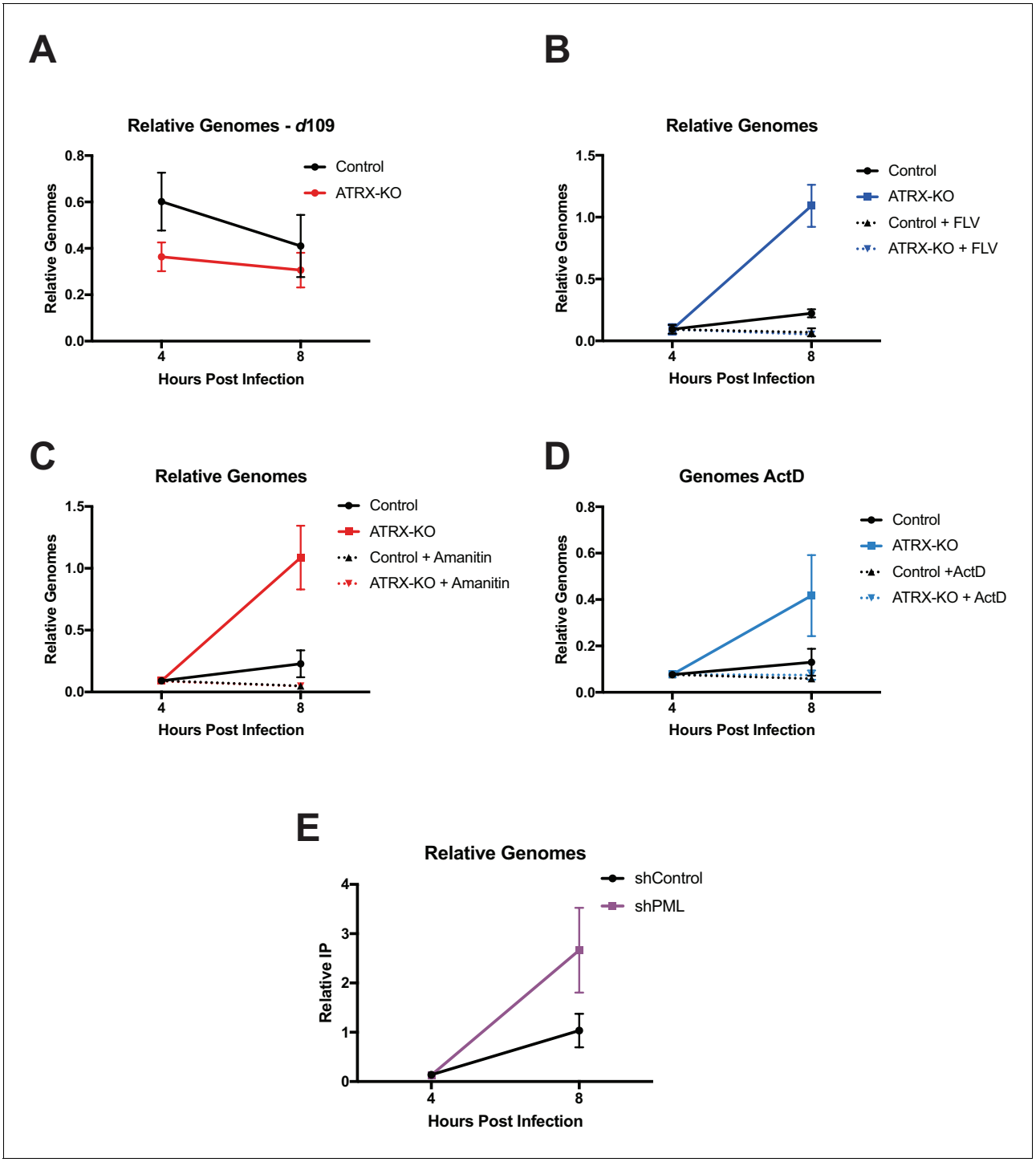

Figure 7—figure supplement 3. Relative HSV genomes during drug treatment. (**A**) Chromatin input for *ICP8* relative to input *GAPDH* to determine relative viral genome copy numbers in cells infected with HSV *d*109. (**B**) Chromatin input for *ICP8* relative to input *GAPDH* to determine relative viral genome copy numbers in the absence or presence of flavopiridol. (**C**) Chromatin input for *ICP8* relative to input *GAPDH* to determine relative viral genome copy numbers in the absence or presence of α-amanitin. (**D**) Chromatin input for *ICP8* relative to input *GAPDH* to determine relative viral genome copy numbers in the absence or presence of ActD. (**E**) Chromatin input for *ICP8* relative to input *GAPDH* to determine relative viral genome copy numbers in cells expressing a control short hairpin or short hairpin against PML.

DOI: https://doi.org/10.7554/eLife.40228.021

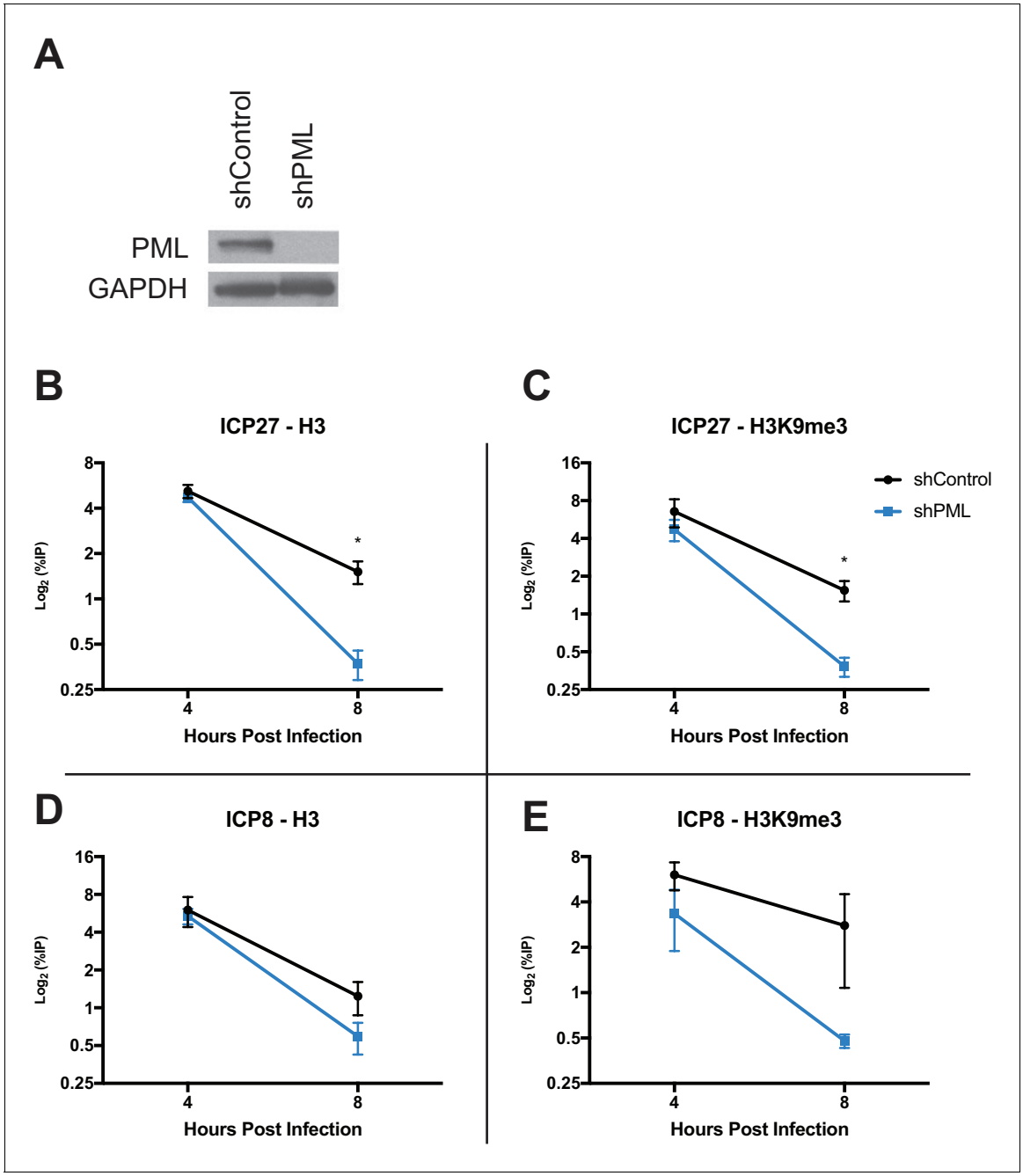

Figure 8. PML promotes maintenance of viral chromatin. (**A**) Immunoblot for PML in shControl and shPML cells. shPML and shControl cells were infected with HSV 7134 at an MOI of 3. Samples were fixed and harvested at 4 and 8 hpi. ChIP-qPCR for (**B**) H3 and (**C**) H3K9me3 at the *ICP27* viral gene promoter. ChIP-qPCR for (**D**) H3 and (**E**) H3K9me3 at the *ICP8* viral gene promoter. ***Figure 8B–E*** are reported as the percent of input immunoprecipitated by each antibody and are the average of 3 independent experiments ± standard error of the mean; two-tailed T test, $p < 0.05$ (*).
DOI: https://doi.org/10.7554/eLife.40228.022

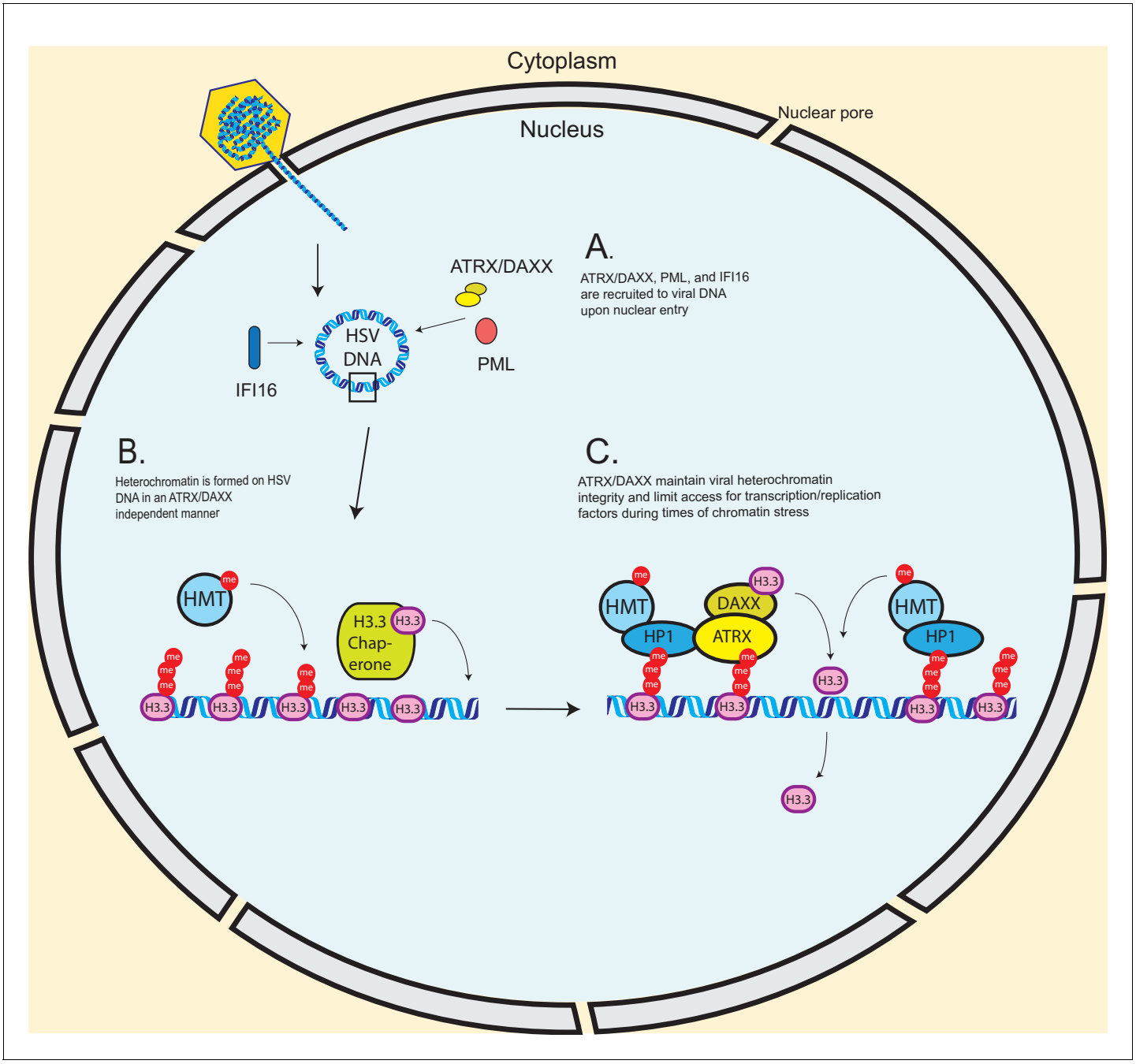

Figure 9. Model – ATRX promotes heterochromatin maintenance during challenges to chromatin stability. (**A**) Incoming HSV genomes are rapidly sensed by IFI16, PML, and ATRX upon nuclear entry. (**B**) The de novo formation of heterochromatin on input viral genomes occurs in an ATRX-independent manner, possibly through a HIRA/ASF1A mediated pathway in conjunction with histone methyltransferases (HMTs). However, our results indicate that ATRX is required to maintain viral heterochromatin stability during destabilizing events such as transcription or replication. (**C**) We hypothesize that ATRX maintains viral heterochromatin integrity resulting in reduced chromatin dynamics, stabilized heterochromatin, and reduced access for transcription factors, viral replication factors, and polymerases.

DOI: https://doi.org/10.7554/eLife.40228.023